Polymer 51 (2010) 2740–2747

Contents lists available at ScienceDirect

Polymer

journal homepage: www.elsevier.com/locate/polymer

Processing-microstructure-property relationship in conductive polymer nanocomposites

Mohammed H. Al-Saleh [a,1], Uttandaraman Sundararaj [a,b,*]

[a] Department of Chemical and Materials Engineering, University of Alberta, Edmonton, Alberta T6G 2G6, Canada
[b] Department of Chemical and Petroleum Engineering, Schulich School of Engineering, University of Calgary, 2500 University Drive N.W., Calgary, Alberta, Canada T2N 1N4

ARTICLE INFO

Article history:
Received 23 December 2009
Received in revised form
7 March 2010
Accepted 13 March 2010
Available online 1 April 2010

Keywords:
Polymer nanocomposites
Processing-microstructure-property relationship
Nanofiller dispersion

ABSTRACT

The processing-microstructure-property relationship in conductive polymer nanocomposites was investigated. Nanocomposites of vapor grown carbon nanofiber (VGCNF)/high density polyethylene (HDPE) with different levels of nanofiber dispersion were formulated by changing the nanocomposites' compounding temperature. Direct (SEM and optical microscopy) and indirect methods (linear viscoelastic properties) were used to characterize the dispersion of nanofiller. VGCNF aspect ratio before and after mixing was measured. Increasing processing temperature was found to increase the nanofiller agglomeration and reduce the breakage of nanofiller because of the decrease in the mixing shear stress and energy. The electrical and electromagnetic interference (EMI) shielding properties of the VGCNF/HDPE nanocomposites decreased with increase in processing temperature from 180 °C to 220 °C because the increase in the agglomeration of VGCNF was more significant than the preservation of the VGCNF aspect ratio. This finding does not mean that the increase in processing temperature will always lead to decrease in the electrical conductivity and EMI shielding properties for all polymer composites. For some composites, it is possible to preserve the filler aspect ratio enough so that the increase in agglomeration is less of a factor.

1. Introduction

Polymer composites based on high aspect ratio nanofillers such as carbon nanotubes and nanofibers are receiving considerable attention because of their unique multifunctional properties at very low filler loading [1–4]. The filler aspect ratio is crucial for many properties such as electrical properties. Electrical properties are the emphasis of this work. The electrical percolation threshold, which is the critical filler concentration that is required to initiate a conductive network within an insulating matrix, is known to decrease with increase in the filler aspect ratio. Percolation thresholds in the range of 0.0021–0.005 wt% were experimentally reported for several multiwall-carbon nanotube (MWCNT)/epoxy nanocomposites [5–8]. Nevertheless, for CNT/thermoplastic nanocomposites, where melt mixing is an industrially preferred processing method [1,9], much higher percolation thresholds have been reported [10–12]. This high threshold is due to the poor dispersion of nanofiller under low shear conditions or to significant degradation of the nanofiller aspect ratio under high shearing conditions.

In addition to the filler aspect ratio, several other factors affect the properties of polymer composites including the polymer properties; the filler intrinsic properties; dispersion, distribution, and orientation of the filler; and adhesion between filler and polymer matrix. Understanding the influence of the these parameters, especially those related to the material's microstructure, on the composite's final properties is of great scientific importance. For conductive polymer composites, there is no direct experimental evidence on the influence of filler dispersion on its final properties. This work focuses on the influence of processing conditions on the filler dispersion and subsequently on the electrical and electromagnetic interference (EMI) shielding properties of conductive polymer nanocomposites, i.e. we study the processing-microstructure-property relationship. To achieve this target we studied the influence of processing temperature on the microstructure, i.e. basically the dispersion and aspect ratio, of high density polyethylene (HDPE)/vapor grown carbon nanofiber (VGCNF) nanocomposite. The dispersion and aspect ratio of carbon nanofiber (CNF) were characterized. CNF dispersion was directly characterized by microscopic techniques and indirectly by utilizing the dynamic rheological analysis technique. Final electrical and EMI

* Corresponding author. Department of Chemical and Petroleum Engineering, Schulich School of Engineering, University of Calgary, 2500 University Drive N.W., Calgary, Alberta, Canada T2N 1N4. Tel.: +1 (403) 220 5750; fax: +1 (403) 284 4852.
E-mail address: u.sundararaj@ucalgary.ca (U. Sundararaj).
[1] Present address: Department of Chemical Engineering, Jordan University of Science and Technology, P.O.Box 3030, Irbid 22110, Jordan.

0032-3861/$ – see front matter © 2010 Elsevier Ltd. All rights reserved.
doi:10.1016/j.polymer.2010.03.022

shielding properties were measured and linked to the nanocomposites' microstructure and processing conditions.

2. Experimental

2.1. Materials and procedure

The constituents of the VGCNF/HDPE nanocomposites formulated in this work were low heat treated (LHT)-Pyrograf III™ carbon nanofibers (PR-24-LHT) produced by Applied Sciences, Inc., Ohio-USA, and the polymer was Nova Chemicals HDPE-19 G polyethylene having an MFI of 1.2 g/10 min (190 °C/2.16 kg) and a specific gravity of 0.962. The polymer was kindly provided by Nova Chemicals.

The VGCNF/HDPE nanocomposites were prepared by melt mixing in a Haake Rheomix series 600 batch mixer (Thermo Scientific, Germany). The mixer is connected to a Rheocord90 control panel. Prior to compounding, the polymer and VGCNF were dried under vacuum for about 16 h at 70 °C and 130 °C, respectively. Mixing was performed at 50 rpm, 9 min (3 min pure polymer melting, 2 min VGCNF feeding and 4 min additional mixing) and 3 different temperatures (180 °C, 200 °C and 220 °C). At the end of mixing, the mixer was turned off and nanocomposites collected and dropped immediately in liquid nitrogen. For electrical conductivity and EMI shielding effectiveness (SE) measurements, a Carver compression molder (Carver Inc., Wabash-IN, USA) was used to prepare two sizes of circular disks; 133 mm and 25.4 mm in diameter and 2 mm in thickness in both cases. The plates were annealed in the molder at 200 °C for 4 min under 18.5 MPa pressure.

2.2. Characterization

2.2.1VGCNF dispersion

The dispersion of VGCNF in the HDPE matrix was quantified by measuring the area of agglomerates in several scanning electron microscopy (SEM) and optical microscopy (OM) micrographs. More details about the characterization methodology can be found within the results and discussion section. For the SEM imaging, a Hitachi S-2700 scanning electron microscope equipped with a Princeton gamma tech (PGA) Imix digital imaging system was used. SEM specimens were fractured in liquid nitrogen and coated with carbon prior to imaging. For OM characterization, the samples were cut at −80 °C with a thickness of 1 μm using Leica cryo-ultramicrotome (EM UC6/FC6). The optical microscope images were taken using ZEISS AXIO Scope A1 microscope.

2.2.2. Nanofibers aspect ratio

Length of VGCNF before and after mixing was characterized by analyzing SEM micrographs of dispersed nanofibers on an Isopore polycarbonate film membrane having an average diameter of 0.4 μm (Isopore, Fisher Scientific). Fig. 1 is a typical example of such micrographs. For the as-received (PR-24-LHT) VGCNF, a small amount of the nanofibers were first dispersed in methanol by sonication. The sonication was carried out for 20 s in a sonicator having an output power of 120 W, or for 1–2 min in a sonicator having an output power of 20 W. Both procedures yielded the same average nanofiber length at the end. A few droplets of the sonicated VGCNF/methanol solution were then filtered on the Isopore membrane. After that, the membrane was placed on an aluminum stub, coated with gold and imaged using the SEM machine described in the above section. Images were taken at two different magnifications in order to consider both the short and long nanofibers. For the characterization of VGCNF length after processing, 10 mg specimens of the VGCNF/HDPE nanocomposites were placed in a Thermogravimetric Analyzer (Pyris 1 TGA, Perkin Elmer, Waltham-MA, USA) to remove the polymer matrix. The specimens were heated, in a nitrogen environment, from 25 °C to 650 °C at a rate of 25 °C/min. The specimens were held for 10 min at 650 °C before cooling. After the polymer matrix was burned off, the nanofibers were collected and dispersed in methanol by sonication for 20 s at 120 W. Then the same procedure used to characterize the length of as-received VGCNF was applied. For each sample, lengths of at least 500 nanofibers were measured.

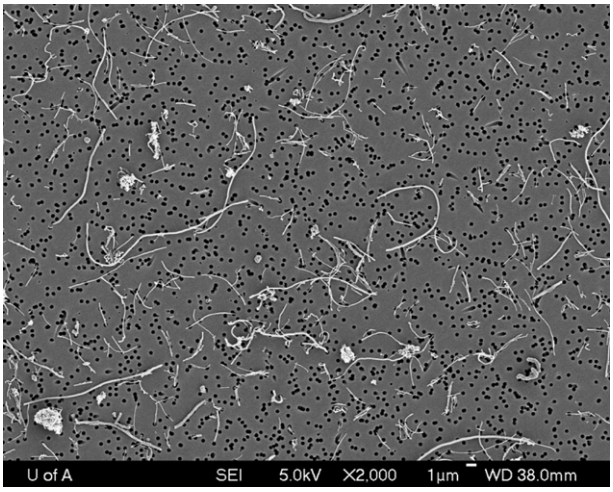

Fig. 1. SEM micrograph of VGCNFs on Isopore polycarbonate film. The black dots are the membrane holes.

2.2.3. Shielding effectiveness

Electromagnetic shielding effectiveness of nanocomposites was measured using the 133 × 2 mm disks prepared by compression molding according to the ASTM D4935-99 standard for planar materials. The set-up used is described in detail elsewhere [13,14]. For each nanocomposite studied, a minimum of two load specimens were tested over a frequency range of 0.1–1.5 GHz. The input power used for all tests was 0 dBm, corresponding to 1 mW.

2.2.4. Electrical conductivity

Electrical conductivity measurements were also conducted on the 133 × 2 mm disks using a Loresta GP resistivity meter (MCP-T610 model, Mitsubishi Chemical Co., Japan) connected with a four-pin probe (MCP-TP08P model, Mitsubishi Chemical Co., Japan). The probe inter-pin spacing is 5 mm and the pin diameter is 2 mm. Five measurements on each face were taken for at least two specimens: the centre of the circular plate (0,0), (0, ±33 mm) and (±33 mm, 0). The average of the readings was reported as the nanocomposite electrical conductivity.

2.2.5. Rheological properties

Rheometrics Inc. RMS800 Rheometer fitted with a 25 mm parallel plate fixture was used to characterize the rheological properties of the nanocomposites and unfilled polymer. The samples were circular discs 25.4 mm in diameter and 2 mm in thickness. The measurements were carried out at 200 °C under nitrogen atmosphere.

3. Results and discussion

3.1. Processing behavior

The rheological behavior of a polymer composite is very sensitive to any change in the composite's microstructure in terms of the dispersion, distribution, orientation and aspect ratio of filler and adhesion between filler and polymer matrix. Even rheological properties of a pure polymer are sensitive to the morphological changes [15,16]. In this study, mixing torque vs. time curves of the

Haake internal mixer and the dynamic rheological properties were used to analyze the influence of processing temperature on the development of the microstructure of the VGCNF/HDPE nanocomposites. In this section, torque vs. time curves of HDPE nanocomposites are presented. The dynamic rheological properties are presented in Section 3.4.

The flow behavior in the Haake mixer is complex owing to the complex geometry of the rotors that allows both shear and extensional mixing. Therefore, estimating the rheological parameters based on the torque and rotation speed is difficult. In this work, it is not our objective to use the Haake mixer torque vs. time curve to obtain some specific rheological parameters. Nevertheless, the objective is to utilize the instantaneous mixing torque readings as an indication of any change in the microstructure of the polymer nanocomposite. For polymer composites, the mixing torque is a measure of the composite viscosity, which in turn is an indication of the composite structure. Increase in mixing torque was interpreted as an indication of better dispersion of clay in different polymer matrices [17,18]. Before discussing the torque vs. time curves, it is worth mentioning that because of the viscous heating effect, the melt temperatures were higher than the mixer wall temperatures (i.e. the set temperatures) by 15 °C. The melt temperatures were measured using a thermocouple in direct contact with the polymer melt inside the mixing chamber. Henceforth, for simplicity, we will refer to the nanocomposites based on their set (i.e. processing) temperature (i.e. the controlled barrel temperature) not their actual melt temperature.

Fig. 2 shows the torque vs. time curves of the 7.5 vol% VGCNF/HDPE nanocomposites as a function of processing temperature. For clarity, the figure does not show the torque curve of the nanocomposite processed at 200 °C since it has the same behavior as the nanocomposites processed at 180 °C and 220 °C with torque readings on average 0.5 Nm lower than those of the 180 °C nanocomposite. The figure has been divided into three distinct processing zones. The first one is the pure polymer melting zone, which starts at 0 s and ends at 180 s. At time 0 s, all polymer pellets were fed to the mixing chamber. In this first zone, polymer was melted before the addition of VGCNF to avoid a severe breakup of nanofibers that would occur if nanofibers were simultaneously added with the solid polymer pellets to the mixer. In the second zone, between 180 s and 300 s, the VGCNFs were gradually added over the 2-min period to avoid overflow problems. The last zone, from 300 s to 540 s, is the nanocomposite compounding (polymer and filler mixing after addition all of the filler).

In the first zone, it is clear that the fusion peak of HDPE decreased with increase in processing temperature. Just before the addition of nanofibers at 180 s, torque readings indicate that HDPE viscosity decreased with increasing the processing temperature from 180 °C to 220 °C. The second processing zone shows the rheological response upon the addition of VGCNF as a function of the processing temperature. The first general observation is the remarkable gradual increase in torque with increasing VGCNF loading. This increase indicates the dependence of VGCNF/HDPE nanocomposite viscosity on the nanofiller loading regardless of the processing temperature. In the 180–220 °C processing zone, the rheological response of nanocomposites to VGCNF addition is identical. Torque increased at a rate of 0.033 Nm/s. Torque reading in this zone is a function of temperature and follows the same trend of unfilled HDPE, i.e. mixing torque decreased by increasing processing temperature from 180 °C to 220 °C.

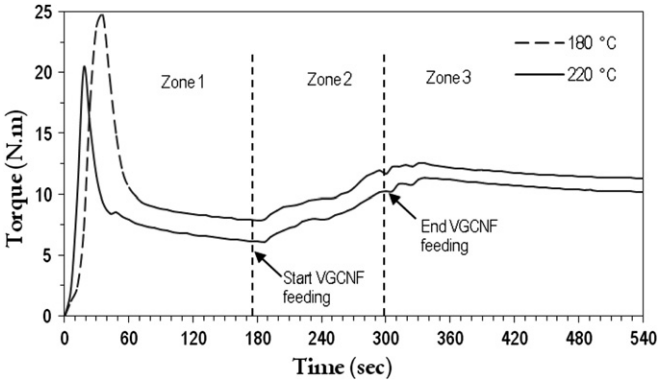

Fig. 2. Torque vs. time curve of VGCNF/HDPE nanocomposites at different operating temperatures. All nanocomposites were mixed at 50 rpm.

3.2. Morphological analysis

Quantifying the state of dispersion of nanofiber in a polymer matrix is technically difficult and has been considered to be one of the major research challenges. In order to get some quantification of the level of VGCNF dispersion, SEM and OM micrographs were analyzed. These techniques give an idea about the percentage of big agglomerates but cannot be used to determine the actual level of dispersion. For each sample, the area of big agglomerates in 10 SEM micrographs taken at a magnification of 1000× was divided by the total area of the 10 images. We noticed that all nanocomposites

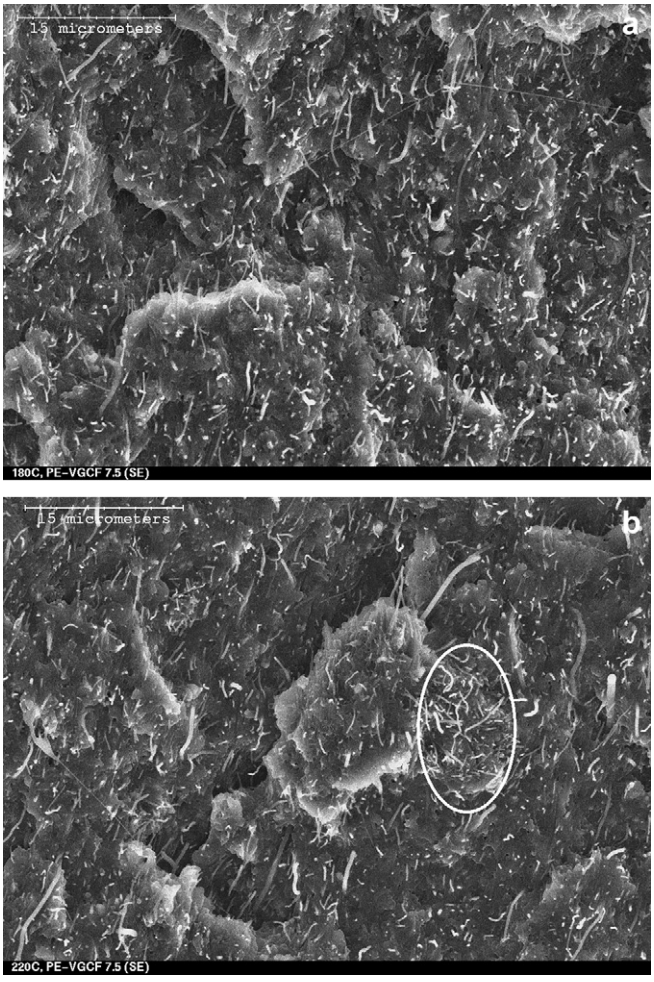

Fig. 3. Effect of processing temperature on the morphology of 7.5 vol% VGCNF/HDPE nanocomposite processed at 50 rpm, 5 min and a) 180 °C and b) 220 °C. All scale bars are 15 μm. The white oval in micrograph b circles a big VGCNF agglomerate.

exhibit a good level of nanofiber dispersion and distribution. However, for the nanocomposite processed at 220 °C, more agglomerates were observed and the area of agglomerates was 3% of the total area of the images analyzed. For the nanocomposites processed at 180 °C and 200 °C, the area of agglomerates was around 1%. Fig. 3 depicts selected SEM micrographs that reflect the general trend (not the actual percents of agglomerates) for the influence of processing temperature on the microstructure of VGCNF/HDPE nanocomposites.

The trend of decreasing VGCNF dispersion with increasing processing temperature and/or decreasing the mixing torque was verified by the analysis of the OM micrographs. The average particle size and the percentage of agglomerates larger than 5 μm in diameter increased from 7.2 μm and 3.6% to 7.7 μm and 4.8%, respectively, with increasing mixing temperature from 180 °C to 220 °C. Fig. 4 depicts the OM images of the nanocomposites processed at 180 °C and 220 °C. VGCNF agglomerates of different sizes can be observed. Some agglomerates are clearly larger than 10 μm in diameter.

3.3. Aspect ratio

The aspect ratio of nanofibers is a crucial parameter that has significant influence on the macro-properties of the nanocomposites. Both the diameter and length of VGCNF were measured.

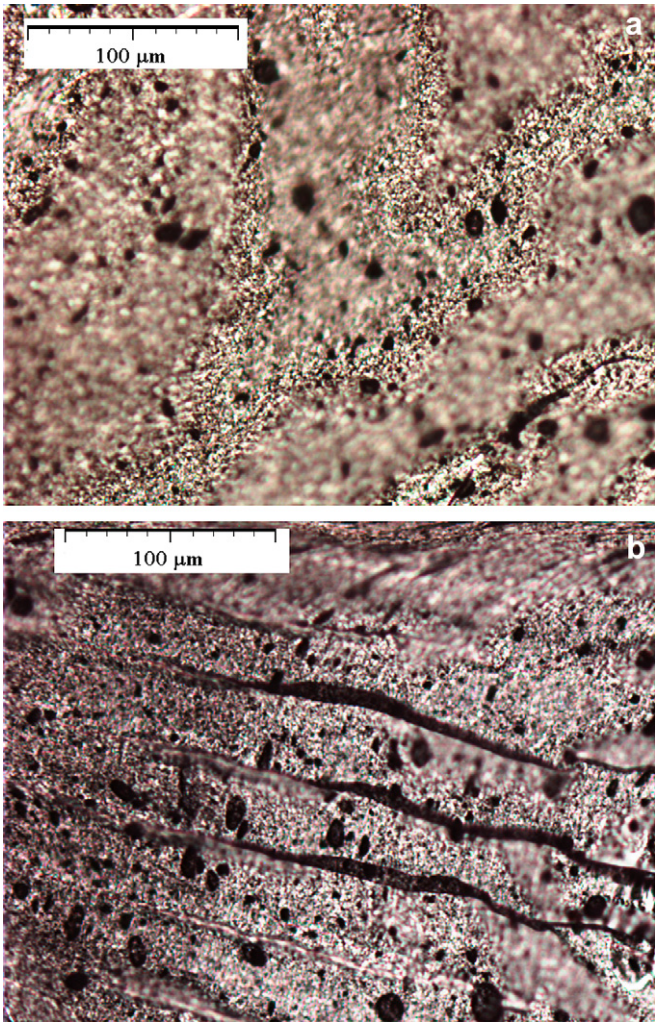

Fig. 4. OM micrographs of VGCNF/HDPE nanocomposites processed at: (a) 180 °C and (b) 220 °C.

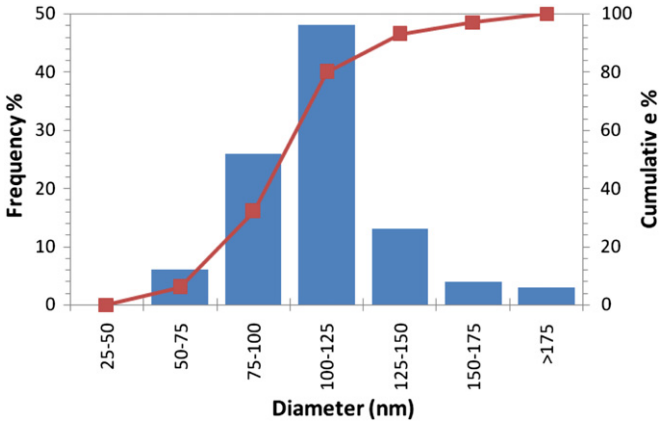

Fig. 5. VGCNF diameter distribution.

The average diameter of the (PR-24-LHT) VGCNF is 110 ± 27 nm. Fig. 5 is a histogram showing the diameter distribution of (PR-24-LHT) VGCNF. It is apparent that 80% of the nanofibers have a diameter smaller than 150 nm. Before mixing, we found that (PR-24-LHT) VGCNF has a number average length of 4.2 ± 4.0 μm. Fig. 6 is a histogram showing the length distribution of VGCNF. It is apparent that the length of most nanofibers is in the range of 2–6 μm Table 1 lists the length and aspect ratio of VGCNF before and after processing with HDPE as a function of processing temperature, mixing energy and mixing torque.

Mixing energy is the mechanical energy consumed to disperse and distribute the nanofiller. For the Haake mixer, mixing energy can be calculated according to Eq. (1).

$$W = \left(2\pi\omega \int_{t_1}^{t_2} \tau dt\right) \Big/ V \tag{1}$$

Where, W is the mixing energy in J/ml, ω is the angular velocity of the rotor (rpm), τ is the torque, t is the time, $\int_{t_1}^{t_2} \tau dt$ is the area under the torque–time curve and V is the volume of the batch (ml). Torque values were recorded every 6 s. The trapezoidal rule was used to find the area under the torque–time curves. Nanofiber length slightly increased with increase in mixing temperature due to the slight decrease in mixing energy and mixing torque, Table 1. Combining the SEM and OM observations with the VGCNF length analysis, it can be concluded that the higher torque readings of the 180 °C nanocomposite compared to the 220 °C nanocomposite is due to the higher viscosity of the HDPE at 180 °C and/or the

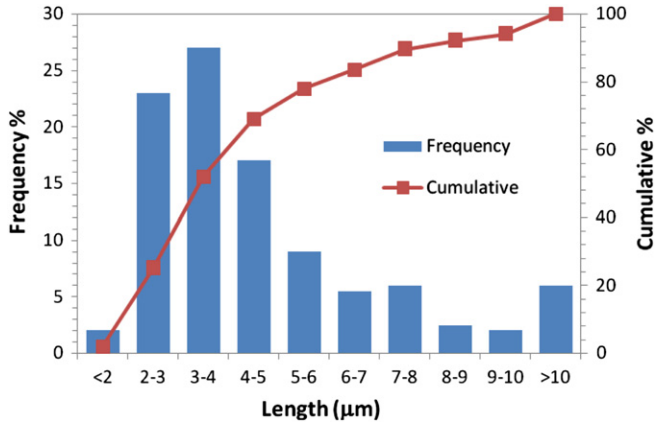

Fig. 6. Length distribution of VGCNF before mixing.

Table 1
Length and aspect ratio of VGCNF before and after mixing with HDPE as a function of processing conditions.

Processing temperature (°C)	Mixing energy (J/ml)	Mixing torque[a] (Nm)	Length number average (μm)	Aspect ratio
Pristine LHT-VGCNF	NA	NA	4.2 ± 4.0	38
180	409	11.3	2.4 ± 2.0	22
200	385	10.8	2.5 ± 1.9	23
220	360	10.2	2.7 ± 1.9	25

[a] Torque reading at the end of mixing.

relatively better dispersion of nanofibers in the 180 °C nanocomposite compared to the 220 °C nanocomposite.

3.4. Dynamic rheological analysis

To complement the Haake Rheomix data and microscopic analysis, dynamic rheological analysis was used. The dynamic rheological analysis was performed on the nanocomposites after processing, i.e. after melt mixing and compression molding. Therefore, it is not expected that this analysis will give information about any instantaneous changes that might happen during processing. However, it is a good probe of the state of the composite microstructure [19–22]. Fig. 7 shows the rheological properties of HDPE and the 7.5 vol% VGCNF/HDPE nanocomposites at 200 °C as function of processing temperature and frequency. For HDPE, it is apparent that processing the polymer between 180 °C and 220 °C has insignificant influence on the polymer rheological properties indicating insignificant influence of temperature on the structure of the pure polymer. This observation is of particular importance since it means that any change in the composites' rheological properties with changing processing temperature should not be attributed to the changes in the polymer rheological properties.

For the 7.5 vol% VGCNF/HDPE nanocomposites, it is apparent that regardless of the processing temperature, all nanocomposites exhibit a strong shear thinning behavior. Whereas, HDPE processed in the range of 180–220 °C show a Newtonian plateau at low frequencies. The 7.5 vol% VGCNF/HDPE nanocomposites have higher η^*, G' and G'' than those of the unfilled polymer. The increase in G', due to addition of VGCNF, is higher than the increase in η^* and G''. This is very clear at low frequencies and diminishes with increasing frequency due to the shear thinning effect. Interestingly, the percent of increase in η^*, G' and G'' decreased with increase in processing temperature. For example at 0.1 rad/s, G' increased by

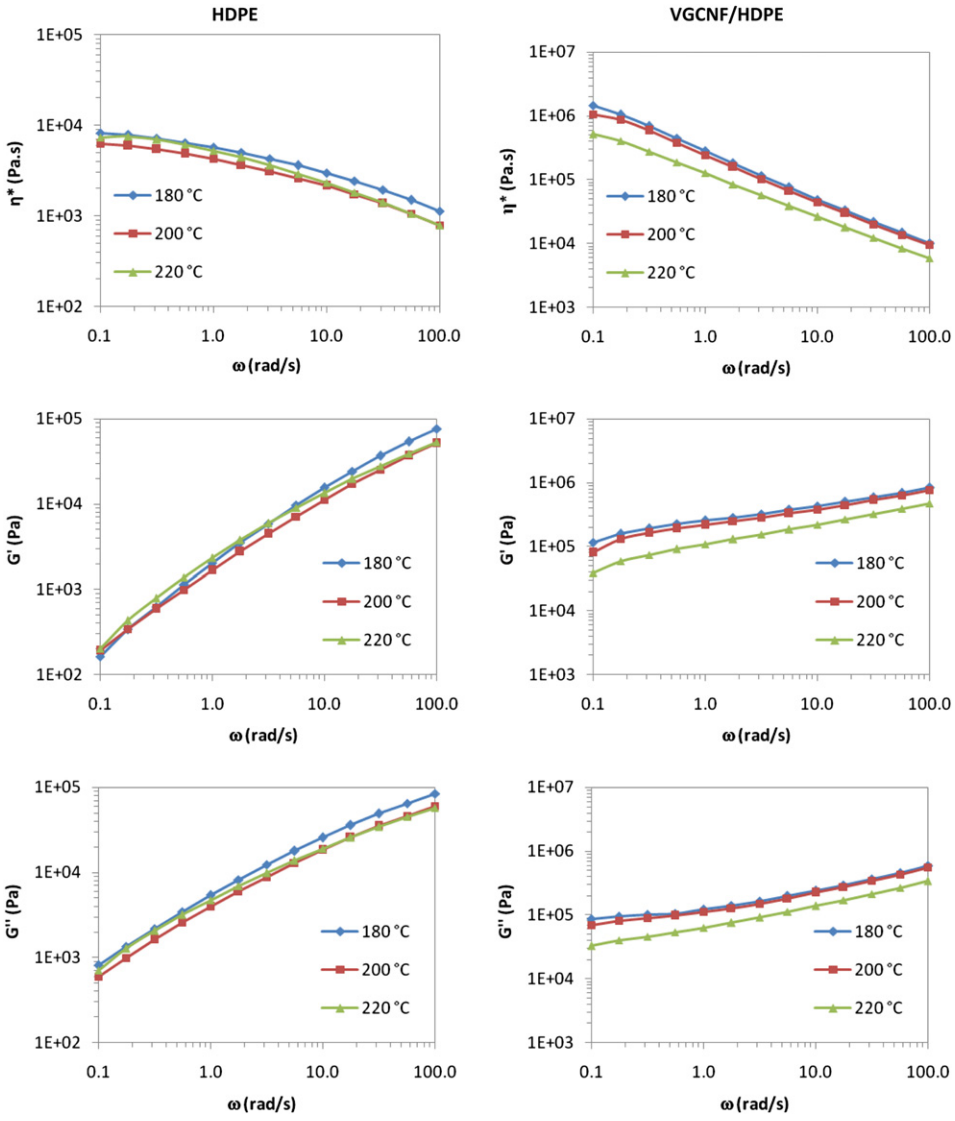

Fig. 7. Rheological parameters of HDPE and 7.5 vol% VGCNF/HDPE nanocomposite at 200 °C as a function of processing temperature and frequency.

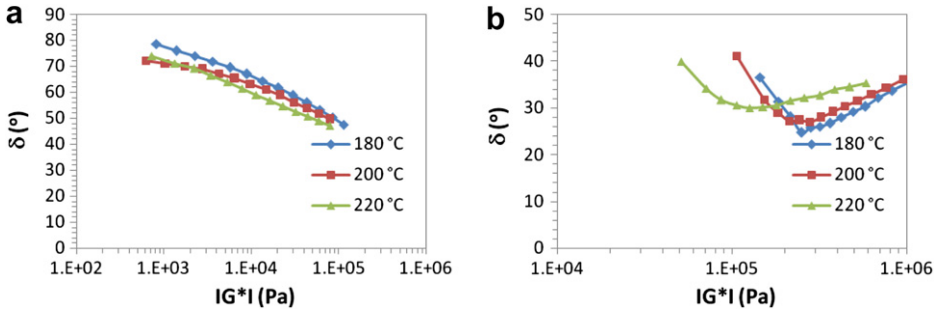

Fig. 8. Phase angle vs. absolute complex modulus (van Gurp–Palmen plot) of: (a) HDPE and (b) 7.5 vol% VGCNF/HDPE nanocomposite as a function of processing temperature.

714%, 419% and 193% for nanocomposites processed at 180 °C, 200 °C and 220 °C, respectively. This remarkable difference in the percent of change in rheological parameters is related to the dissimilar microstructures.

Fig. 8 shows the phase angle (δ) vs. absolute value of complex modulus (IG^*I) of the unfilled HDPE and VGCNF/HDPE nanocomposite. This figure is known as van Gurp–Palmen plot. It was first introduced by van-Grup and Palmen [23] to verify the time–temperature superposition principle (TTS) in polymer blends. By plotting the δ vs. IG^*I the influence of shifting along the frequency axis is eliminated. Thus, the isothermal δ vs. IG^*I curves should coincide if TTS holds [23,24]. This plot was later used by many researchers to detect the rheological percolation threshold in polymer nanocomposites [10,19,25,26]. Herein, we will use this plot to detect the change in the structure of the unfilled HDPE and VGCNF/HDPE nanocomposites with changing processing temperature. For unfilled HDPE, Fig. 8a, δ is seen to decrease with increase in IG^*I regardless the processing temperature. At a given IG^*I, δ marginally decreased with increase in processing temperature indicating insignificant change in the polymer structure. For the nanocomposites, an interesting behavior of the δ vs. IG^*I curves can be observed. The phase angle decreased with increasing IG^*I, reached an inflection point (a minimum value (δ_{min}), then started to increase with increasing IG^*I. Similar behavior at a very high carbon black (CB) loading (9 and 13 vol%) were reported for CB/polypropylene composite [27]. The δ_{min} decreased with decrease in the nanocomposite processing temperature. Moreover, there is a significant shift in the δ vs. IG^*I curves. A shift in the δ vs. IG^*I curves with increasing filler loading was reported for many nanocomposites [10,25–28]. Thus, the shift is a clear indication of the change in nanofiller dispersion with changing the processing temperature.

The difference in microstructure can also be confirmed from the G' vs. G'' plot. Different slopes of the G' vs. G'' curves were used as an indication of change in morphology of homopolymer, copolymer and polymer composites and blends [20,29–31]. Fig. 9 depicts the G' vs. G'' curves of the VGCNF/HDPE nanocomposites. Four major observations can be drawn from the figure. The first clear observation is that for each nanocomposite, G' is higher than G''; notice that all curves are above $y = x$ line. The second observation is the shift in the G' vs. G'' curves towards higher G' and G'' with decreasing nanocomposite processing temperature. The third interesting observation is that, for each nanocomposite, there is an inflection point at which the slope of the G' vs. G'' curves remarkably decrease, i.e. the rate of increase in G'/rate of increase in G''($\Delta G'/\Delta G''$), decreases with increase in frequency. In our curves this point happens at a frequency of 0.56 rad/s. For example, the slope of the G' vs. G'' curve for the 180 °C nanocomposite is 4.8 in the frequency range of 0.1–0.56 rad/s and decreased to 1.2 in the frequency range 0.56–100 rad/s. The last observation is that the slope of the G' vs. G'' curves at low frequencies was found 4.8, 4.1 and 2.7 for nanocomposites processed at 180 °C, 200 °C, and 220 °C, i.e. the slope decreased with increasing processing temperature. However, at higher frequencies, the change in the slope of G' vs. G'' curves with increasing processing temperature was insignificant. The slope of the 180 °C and 220 °C G' vs. G'' curves was 1.2 and 1.3, respectively. For the unfilled HDPE, not shown in the figure, the G' vs. G'' curves almost coincided because of the insignificant influence of processing temperature on the unfilled polymer structure. In the low frequency region, the slope of the G' vs. G'' curves was 0.37, 0.41 and 0.47 for unfilled polymer processed at 180 °C, 200 and 220 °C, respectively.

It might be argued that the increase in the slope of the G' vs. G'' curves cannot be considered an indication of enhancement of nanofibers dispersion based on some reports in which it was mentioned that for MWCNT/polycarbonate [20] and MWCNT/linear medium density PE [11] the slope of the G' vs. G'' curves decreased with increase in the nanofiller content. The increase in the nanofiller content can be assumed as enhancement in the nanofiller dispersion. It is apparent that the previous works [11,20] were referring to the slope of the G' vs. G'' curves as it appears on the logarithmic scale, i.e. the slope of the log G' vs. log G'' plot. The slope of the log G' vs. log G'' does not reflect the actual rate of increase in G'/rate of increase in G'' with increasing frequency. $(\log A - \log B)/(\log C - \log D)$ is not proportional to $(A - B)/(C - D)$.

To verify the relation between filler concentration and the slope of G' vs. G'' curve we utilized set of data previously reported for PC nanocomposites filled with 0–2 wt% MWCNT [25]. The nanocomposites were prepared by melt mixing in a DACA microcompounder, Miniature Batch Mixer (MBM) and Alberta Polymer Asymmetric Minimixer (APAM). Fig. 10 shows the G' vs. G'' of MWCNT/PC nanocomposites prepared using the DACA microcompounder. It is apparent that for a certain G'', G' increases with increase in MWCNT content. In addition, it may be inferred from the

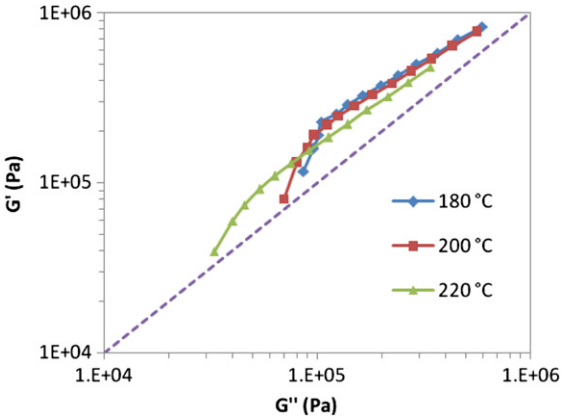

Fig. 9. G' vs. G'' curves of VGCNF/HDPE nanocomposites as function of processing temperature.

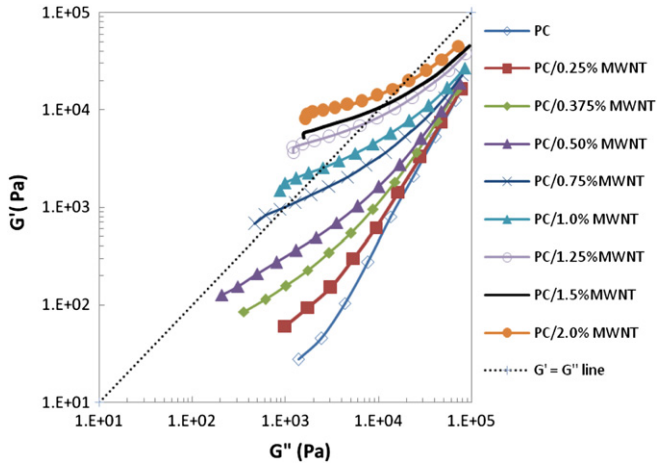

Fig. 10. G' vs. G'' of MWCNT/PC nanocomposites as a function of MWCNT content. All amounts are in wt%.

figure that the slope of the log G' vs. log G'' decreases with increase in filler concentration. Nevertheless, for the slope of the G' vs. G'' we found that the slope increases with increasing filler concentration as shown in Fig. 11. The figure shows that at both low and high frequencies the slope of G' vs. G'' curves increases with increase in MWCNT concentration. The increase of slope with increasing MWCNT concentration is more pronounced at low frequencies. Similar behaviors were found for the nanocomposites prepared by the APAM and MBM mixers.

Rheological properties of a polymer composite are function of the filler aspect ratio, filler concentration, degree of dispersion, distribution and orientation, adhesion between the filler and polymer matrix and polymer matrix rheological properties. For the nanocomposites processed in the range of 180–220 °C, all these factors are constant or can be safely assumed constant except the degree dispersion of the filler. Based on this, it can be concluded that the decrease in the nanocomposite η^*, G' and G'' values, the shift and increase in δ_{min} on the van Gurp–Palmen plots, the shift of the δ vs. IG^*I curves and the shift and decrease in slope of the G' vs. G'' curves and the shift with increasing processing temperature from 180 °C to 220 °C is an indication of increase in agglomeration of nanofibers. This conclusion is in agreement with the OM and SEM characterization. This experimental observation is direct evidence that rheological properties can be used to quantify the degree of filler dispersion when the other influencing factors mentioned above are insignificant.

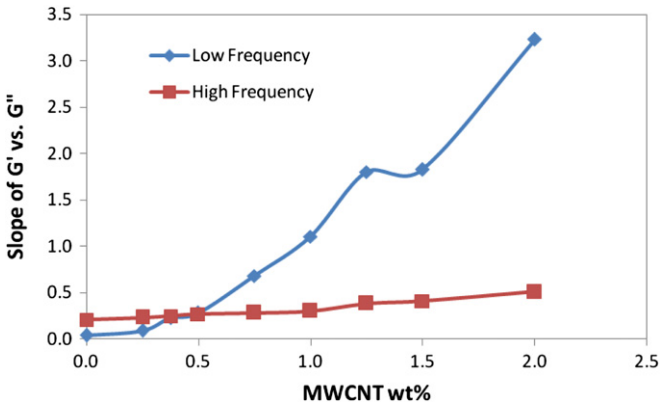

Fig. 11. Slope of the G' vs. G'' curves of MWCNT/PC nanocomposites at low and high frequencies as a function of MWCNT concentration.

3.5. Electrical conductivity and EMI SE

Electrical conductivity and EMI SE are related properties, i.e. EMI SE increases with increase in electrical conductivity. Factors leading to higher electrical conductivity, such as higher aspect ratio and better dispersion of the filler, will also lead to higher EMI SE. Fig. 12 shows the effect of processing temperature on the electrical conductivity (σ) and EMI SE of the HDPE nanocomposites. The EMI SE results reported in Fig. 12 are the average shielding values of 2 mm thick plate nanocomposites in the 0.1–1.5 GHz frequency range. Within 0.1–1.5 GHz, EMI SE was almost independent of frequency. It is apparent that with increasing processing temperature there is a considerable decrease in the nanocomposite's electrical conductivity and EMI SE. For example, the EMI SE of nanocomposites decreased by 24% from 29.5 dB to 22.5 dB with increasing mixing temperature from 180 °C to 220 °C. With increase in processing temperature the nanofiller aspect ratio slightly increased and the nanofibers degree of dispersion decreased. Thus, the remarkable decrease in electrical conductivity and EMI SE properties with the increase processing temperature is undoubtedly related to the decreases in nanofiber dispersion. This observation can be used as a proof that electrical properties can be used to quantify the level of filler dispersion if other influencing factors are constant.

The results reported in Fig. 12 do not mean that for fiber-filled composites the increase in processing temperature will always lead to decrease in composites electrical conductivity and EMI SE. It is expected that the increase in processing temperature will most likely be associated with decrease in fiber dispersion and increases in fiber aspect ratio due to the decrease in mixing torque. Thus, depending on the filler degree of dispersion and aspect ratio after mixing, the increase in mixing temperature could decrease, increase or have no effect on final properties. For example, for carbon fiber/polymer composites, an increase in electrical conductivity was reported with increase in processing temperature [32,33] apparently because the reduction in fiber breakage was more significant than the increase in agglomeration. For CNT/polyamide 6 and CNT/polyamide 6,6, an enhancement in electrical conductivity of the nanocomposites was found with increasing processing temperature [9]. The authors related the increase in electrical conductivity to the enhancement in CNT dispersion with increasing mixing temperature. The decrease in polymer viscosity that was associated with the increase in processing temperature was claimed to facilitates the diffusion of polymer chains into the

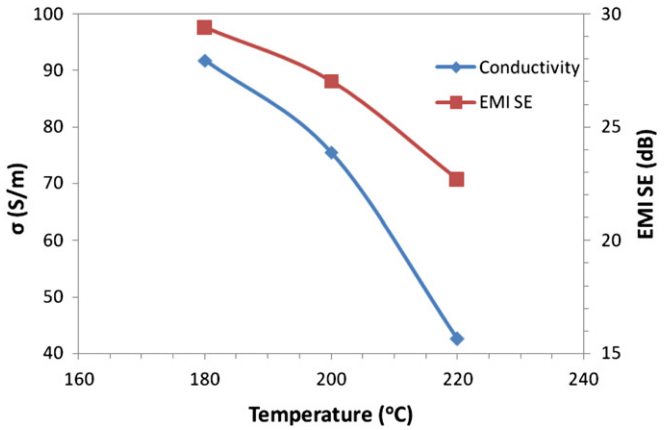

Fig. 12. Effect of processing temperature on the electrical conductivity and EMI SE of 2 mm thick plates in the 0.1–1.5 GHz frequency range of 7.5 vol% VGCNF/HDPE. Operating conditions: 50 rpm and 5 min

primary aggregates and consequently increases the erosion from the CNT agglomerates and thus enhances the dispersion of CNT [9]. Unfortunately, no characterization of CNT dispersion as a function of processing temperature was provided in the work to support this analysis. Nevertheless, we believe that the increase in CNT/PA 6 and PA 66 nanocomposites electrical conductivity with increasing processing temperature was for the same reason we stated above for CF/polymer composites.

4. Conclusions

Influence of processing conditions on the microstructure and subsequently on the electrical and EMI shielding properties of conductive polymer nanocomposites has been elaborated. Polymer nanocomposites of VGCNF/HDPE were melt mixed at different temperatures in order to obtain different microstructures. The microstructure was qualitatively evaluated in terms of nanofiber dispersion and aspect ratio. Increasing the processing temperature from 180 °C to 220 °C was found to increase the nanofiber agglomeration, as it was observed by analyzing the SEM and OM micrographs (the direct characterization) and the decrease in the η^*, G' and G'' values (the indirect characterization), because of the decrease in the melt mixing shear stress and energy. The nanofiber aspect ratio marginally maintained with increasing processing temperature. Thus, the electrical and EMI shielding properties of VGCNF/HDPE nanocomposites decreased with increasing processing temperature from 180 °C to 220 °C, indicating that the nanocomposites electrical and EMI shielding properties degrade with increase in nanofiller agglomeration.

No general rule can be given for the influence of processing temperature on the conductive nanocomposite properties. Increasing processing temperature might decrease, increase or have no influence on final properties. All depend on the microstructure (dispersion vs. aspect ratio) that will be developed as a result of changing the processing temperature. Typically with increasing processing temperature, polymer melt viscosity decreases and consequently mixing torque and energy decrease. The decrease in mixing torque and energy will be associated with increase in nanofiber agglomeration and preservation of nanofiller aspect ratio. It is the balance of these two factors that will decide the nanocomposite final properties. For example, if the preservation of nanofiller aspect ratio was more significant than the increase in nanofiber agglomeration, then increasing processing temperature will enhance the nanocomposite's electrical and EMI shielding properties.

In this article, in addition to the results relating the processing, microstructure, and properties, we present new rheological parameters that are very sensitive to the change in the nanocomposites microstructure; namely, the slope and shift in G'/G'' curves and the shape and shift of the phase angle vs. complex modulus curves (van Gurp–Palmen curves). We found that with increase in nanofiller dispersion, the G'/G'' curves shifted towards higher G' and G'' values and the slope of the G'/G'' increased. This increase was very remarkable at very low frequencies. For the van Gurp–Palmen plots, it was found that with increasing dispersion, the δ vs. IG^*I shifted towards lower δ and higher IG^*I. Moreover, δ vs. IG^*I also showed a V or U shape in which the minimum δ value was found to decrease with increase in filler dispersion.

Acknowledgments

The authors thank the Natural Sciences and Engineering Research Council of Canada (NSERC) for the financial support of this work. We gratefully acknowledge Dr. Bin Lin for helping with OM analysis and G. Braybrook for the collection of SEM images.

References

[1] Al-Saleh MH, Sundararaj U. Carbon 2009;47(1):2–22.
[2] Breuer O, Sundararaj U. Polymer Composites 2004;25(6):630–45.
[3] Moniruzzaman M, Winey KI. Macromolecules 2006;39(16):5194–205.
[4] Winey KI, Kashiwagi T, Mu M. MRS Bulletin 2007;32(4):348–53.
[5] Sandler JKW, Kirk JE, Kinloch IA, Shaffer MSP, Windle AH. Polymer 2003;44 (19):5893–9.
[6] Bauhofer W, Kovacs JZ. Composites Science and Technology 2009;69 (10):1486–98.
[7] Bryning MB, Islam MF, Kikkawa JM, Yodh AG. Advanced Materials 2005;17 (9):1186–91.
[8] Martin CA, Sandler JKW, Shaffer MSP, Schwarz MK, Bauhofer W, Schulte K, et al. Composites Science and Technology 2004;64(15):2309–16.
[9] Krause B, Pötschke P, Häußler L. Composites Science and Technology 2009;69 (10):1505–15.
[10] Meincke O, Kaempfer D, Weickmann H, Friedrich C, Vathauer M, Warth H. Polymer 2004;45(3):739–48.
[11] McNally T, Pötschke P, Halley P, Murphy M, Martin D, Bell SEJ, et al. Polymer 2005;46(19):8222–32.
[12] Zhou Z, Wang SF, Zhang Y, Zhang YX. Journal of Applied Polymer Science 2006;102(5):4823–30.
[13] Al-Saleh MH, Sundararaj U. Polymers for Advanced Technologies; 2009;. doi:10.1002/pat.1526.
[14] Al-Saleh MH, Sundararaj U. Macromolecular Materials and Engineering 2008;293(7):621–30.
[15] Hussein IA, Williams MC. Macromolecular Rapid Communications 1998;19 (6):323–5.
[16] Shenoy AV. Rheology of filled polymer systems. Springer-Verlag; 1999.
[17] Durmus A, Kasgoz A, Macosko CW. Polymer 2007;48(15):4492–502.
[18] Artzi N, Narkis M, Siegmann A. Journal of Polymer Science Part B: Polymer Physics 2005;43(15):1931–43.
[19] Pötschke P, Abdel-Goad M, Alig I, Dudkin S, Lellinger D. Polymer 2004;45 (26):8863–70.
[20] Potschke P, Fornes TD, Paul DR. Polymer 2002;43(11):3247–55.
[21] Du F, Scogna RC, Zhou W, Brand S, Fischer JE, Winey KI. Macromolecules 2004;37(24):9048–55.
[22] Vermant J, Ceccia S, Dolgovskij MK, Maffettone PL, Macosko CW. Journal of Rheology 2007;51(3):429–50.
[23] van Gurp M, Palmen J. Rheology Bulletin 1998;67(1):5–8.
[24] Trinkle S, Friedrich C. Rheologica Acta 2001;40(4):322–8.
[25] Lin B, Sundararaj U, Potschke P. Macromolecular Materials and Engineering 2006;291(3):227–38.
[26] Valentino O, Sarno M, Rainone NG, Nobile MR, Ciambelli P, Neitzert HC, et al. Physica E: Low-dimensional Systems and Nanostructures 2008;40(7):2440–5.
[27] Chen G, Yang B, Guo S. Journal of Polymer Science Part B: Polymer Physics 2009;47(18):1762–71.
[28] Prashantha K, Soulestin J, Lacrampe MF, Krawczak P, Dupin G, Claes M. Composites Science and Technology 2009;69(11–12):1756–63.
[29] Chuang H-K, Han CD. Journal of Applied Polymer Science 1984;29 (6):2205–29.
[30] Han CD, Kim J, Kim JK. Macromolecules 1989;22(1):383–94.
[31] Harrell ER, Nakajima N. Journal of Applied Polymer Science 1984;29 (3):995–1010.
[32] Das NC, Chaki TK, Khastgir D. Carbon 2002;40(6):807–16.
[33] Chiang WY, Cheng KY. Polymer Composites 1997;18(6):748–56.